Cureus
Part of SPRINGER NATURE

Open Access Case Report

# An Unusual Thoracic Presentation of Multiple Myeloma: Rib-Based Paraskeletal Plasmacytoma Mimicking a Lung Mass

**Review began** 10/10/2026
**Review ended** 10/17/2026
**Published** 10/21/2026

© **Copyright** 2026
Rondón-Carvajal et al. This is an open access article distributed under the terms of the Creative Commons Attribution License CC-BY 4.0., which permits unrestricted use, distribution, and reproduction in any medium, provided the original author and source are credited.

**DOI:** 10.7759/cureus.118321

Julián Rondón-Carvajal [1], Elena Useche-Henao [2], María José Espir-Sánchez [2], Yineth Agudelo-Zapata [3]

1. Internal Medicine - Pulmonology, Universidad CES, Medellín, COL 2. Internal Medicine, Universidad CES, Medellín, COL 3. Internal Medicine, Hospital General de Medellín, Medellín, COL

**Corresponding author:** Julián Rondón-Carvajal, julianrondoncarvajal@gmail.com

## Abstract

Thoracic plasma cell neoplasms may be difficult to classify when they arise at the interface between the ribs, pleura, and lung. We report a 75-year-old male who presented with a five-month history of progressive right arm pain, functional limitation, and constitutional symptoms. Chest computed tomography revealed an osteolytic lesion centered in the right eighth rib, with a costal/extrapleural mass (6.0 × 3.5 cm) and, on MRI, extended to the adjacent vertebral body with a soft-tissue component and additional osteolytic lesions. Laboratory evaluation showed severe normocytic anemia, an increase in serum creatinine from a baseline of 0.7 mg/dL to 1.3 mg/dL, and an IgA-kappa monoclonal component. Biopsy of the rib lesion demonstrated a CD38-positive, kappa-restricted plasma cell neoplasm, while bone marrow showed 30% clonal plasma cells on trephine CD138 immunohistochemistry (15.9% by flow cytometry). The presence of clonal bone marrow involvement, severe anemia, and multifocal osteolytic disease established the diagnosis of active multiple myeloma presenting with a rib-based plasmacytoma and extrapleural paraskeletal soft-tissue component abutting the pleura, rather than a primary pulmonary or solitary bone plasmacytoma. Bortezomib, lenalidomide, and dexamethasone (VRd) induction was planned but could not be started because of competing surgical priorities and drug unavailability; the patient died 67 days after admission from progressive disease with refractory hypercalcemia. This case highlights the importance of integrating the anatomical origin of the lesion with histopathological, monoclonal protein, bone marrow, and systemic imaging findings to avoid diagnostic misclassification and guide appropriate treatment.

**Categories:** Hematology, Pathology, Pulmonology
**Keywords:** contrast-enhanced ct thorax, extramedullary multiple myeloma, extramedullary plasmacytoma (emp), hemato-oncology, plasma cell malignancy, thoracic radiology

## Introduction

Plasma cell neoplasms other than multiple myeloma (MM) are uncommon, since MM accounts for more than 95% of cases; solitary bone plasmacytoma (SBP) most frequently involves the spine, followed by the pelvis and the ribs, whereas true extramedullary disease without contact with bone is reported in only 0.5-4.8% of patients with newly diagnosed MM, so most thoracic plasma cell masses in MM are rib-based paraskeletal lesions. SBP and extramedullary plasmacytoma are defined by a biopsy-proven clonal plasma cell lesion without additional osteolytic lesions or myeloma-defining events. In contrast, bone marrow infiltration of 10% or greater accompanied by anemia, renal impairment, hypercalcemia, bone lesions, or another validated myeloma-defining event supports the diagnosis of active MM [1,2].

Thoracic plasma cell tumors may be difficult to classify when they arise at the interface between the ribs, pleura, and lung. A rib-based lesion may extend into adjacent soft tissues and resemble a primary pulmonary mass; however, this paraskeletal extension differs from true extramedullary disease without direct contact with bone [3]. Computed tomography helps identify the anatomical origin of the lesion, while whole-body imaging may detect additional skeletal involvement and establish systemic disease [4,5]. We report a case of a 75-year-old male with an osteolytic lesion arising from the right eighth rib and a pleuropulmonary soft-tissue component. Additional lytic lesions, severe anemia, an IgA-kappa monoclonal component, and 30% clonal plasma cells on trephine CD138 immunohistochemistry (15.9% by flow cytometry) established the diagnosis of MM presenting with a rib-based plasmacytoma and contiguous pleuropulmonary extension. This case highlights the importance of integrating imaging, histopathology, and systemic evaluation to avoid diagnostic misclassification.

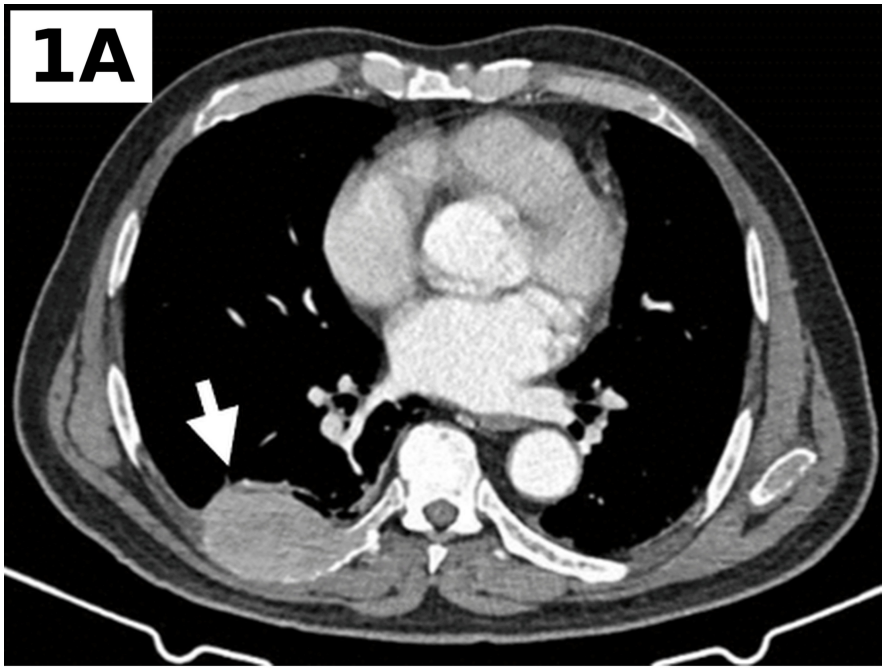
## Case Presentation

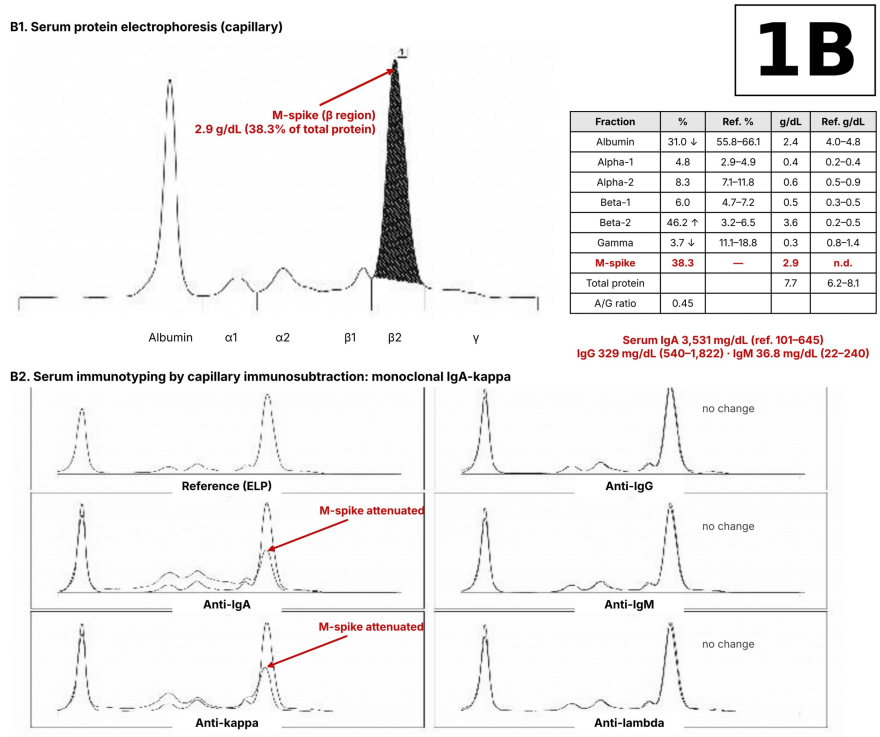
A 75-year-old male presented with a five-month history of pain in the medial aspect of the right arm, associated with functional limitation and constitutional symptoms. On examination, breath sounds were decreased at the right lung base, and active and passive movements of the right shoulder were severely limited by pain, without motor or sensory deficit. A skeletal survey revealed a 5-cm lytic lesion of the proximal right humerus with circumferential cortical thinning and an associated pathological fracture,

accounting for the upper-limb impairment. He denied dyspnea or hemoptysis.

Admission calcium level was 10.4 mg/dL with serum albumin of 2.4 g/dL, giving an albumin-corrected calcium of 11.7 mg/dL; 10 days into their hospital stay, total calcium was 11.7 mg/dL (corrected 13.0 mg/dL), with suppressed parathyroid hormone (PTH) (8.29 pg/mL). Renal impairment (creatinine: 1.3 mg/dL; blood urea nitrogen: 20 mg/dL), non-nephrotic-range proteinuria, and severe normocytic anemia (hemoglobin: 7.8 g/dL; mean corpuscular volume: 91 fL) were documented.

Contrast-enhanced chest computed tomography (CT) revealed a 6 cm osteolytic lesion with an associated soft-tissue component in the posterior segment of the right eighth rib (Figure *1A*), together with additional lytic lesions at other skeletal sites. Serum protein electrophoresis and immunofixation demonstrated a monoclonal IgA-kappa component (Figure *1B*), and bone marrow showed 30% clonal plasma cells on trephine CD138 immunohistochemistry (15.9% by flow cytometry). While borderline calcium and acute-on-chronic creatinine elevation were observed, the myeloma-defining events meeting International Myeloma Working Group (IMWG) CRAB (hypercalcemia (C), renal impairment (R), anemia (A), and bone lesions (B)) criteria were severe normocytic anemia (hemoglobin: 7.8 g/dL) and polyostotic osteolytic lesions [2].




| Fraction | % | Ref. % | g/dL | Ref. g/dL |
|---|---|---|---|---|
| Albumin | 31.0 ↓ | 55.8–66.1 | 2.4 | 4.0–4.8 |
| Alpha-1 | 4.8 | 2.9–4.9 | 0.4 | 0.2–0.4 |
| Alpha-2 | 8.3 | 7.1–11.8 | 0.6 | 0.5–0.9 |
| Beta-1 | 6.0 | 4.7–7.2 | 0.5 | 0.3–0.5 |
| Beta-2 | 46.2 ↑ | 3.2–6.5 | 3.6 | 0.2–0.5 |
| Gamma | 3.7 ↓ | 11.1–18.8 | 0.3 | 0.8–1.4 |
| M-spike | 38.3 | — | 2.9 | n.d. |
| Total protein | | | 7.7 | 6.2–8.1 |
| A/G ratio | 0.45 | | | |

**FIGURE 1: Initial investigations for multiple myeloma.**

(A) Contrast-enhanced chest CT scan showing the borderline costal lesion (white arrow); the lesion was costal/extrapleural (6.0 × 3.5 cm).

(B) Monoclonal protein studies. (B1) Capillary serum protein electrophoresis showing a monoclonal peak (M-spike, arrow) in the β region of 2.9 g/dL (38.3% of total protein 7.7 g/dL), with hypoalbuminemia (2.4 g/dL) and suppressed γ-globulins (0.3 g/dL). (B2) Capillary immunosubtraction: the M-spike is attenuated by anti-IgA and anti-kappa antisera but not by anti-IgG, anti-IgM, or anti-lambda, identifying a monoclonal IgA-kappa protein. Serum IgA: 3,531 mg/dL (reference: 101–645); IgG: 329 mg/dL (540–1,822); IgM: 36.8 mg/dL (22–240).

ELP: serum protein electrophoresis.

CT- and ultrasound-guided core biopsy of the 54 × 37 mm right posterior costal lesion yielded four core fragments (largest 10 mm). Histology showed a hypercellular, diffuse, sheet-like, and loosely cohesive

infiltrate of plasmacytoid cells that effaced the sampled tissue, without intervening normal architecture. The cells had moderately abundant cytoplasm and eccentrically placed round nuclei with dense, coarsely clumped chromatin, and intranuclear inclusions (Dutcher bodies) were identified; conspicuous nucleoli, occasional binucleated forms, and mild-to-moderate nuclear pleomorphism were also present. Together with a Ki-67 index of approximately 60%, these features indicate a mature-to-intermediate-grade plasma cell neoplasm with high proliferative activity. Radiologically, the lesion was expansile and destructive, measuring 6.0 × 3.5 cm on CT and 59 × 38 × 38 mm on MRI, with cortical destruction, an enhancing soft-tissue component, and extension into the adjacent vertebral body, consistent with an infiltrative rather than circumscribed growth pattern.

Percutaneous biopsy of the rib lesion confirmed a plasma cell neoplasm (Figure *2*). By immunohistochemistry, the neoplastic cells were diffusely positive for CD138 and CD38, showed monotypic kappa light-chain expression with lambda negativity, and were negative for pan-cytokeratin, CD45 (leucocyte common antigen), CD20, and CD3; the Ki-67 proliferation index was approximately 60%. The bone marrow trephine showed CD138-positive, kappa-monotypic plasma cells that were CD56- and cyclin D1-negative, confirming the plasma cell lineage and clonal identity across sites. Given the polyostotic osteolytic pattern, the fulfillment of CRAB criteria, and the absence of the endobronchial or mediastinal/hilar lymph node involvement that typifies primary pulmonary plasmacytoma (PPP), the case was classified as MM with an underlying costal SBP rather than PPP [1,2]. Table *1* presents a timeline of the diagnostic evaluation mapped against the criteria applied at each step.

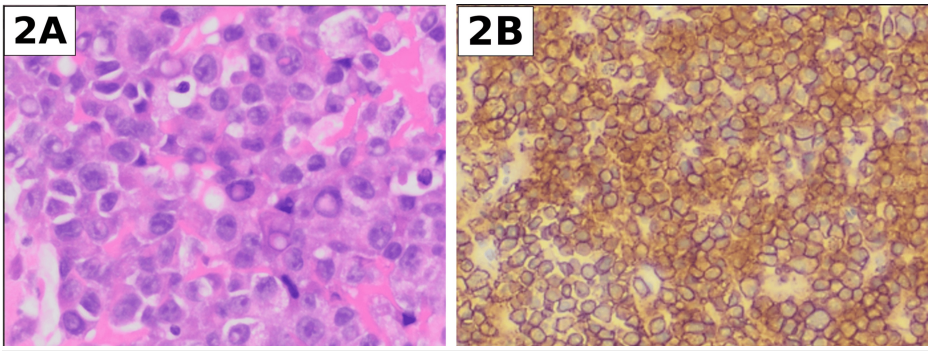



**FIGURE 2: Confirmatory investigations for multiple myeloma.**

(A) Hematoxylin and eosin (H&E) staining, ×400: Histology showed a hypercellular, diffuse, sheet-like, and loosely cohesive infiltrate of plasmacytoid cells that effaced the sampled tissue, without intervening normal architecture. The cells had moderately abundant cytoplasm and eccentrically placed round nuclei with dense, coarsely clumped chromatin, and intranuclear inclusions (Dutcher bodies) were identified.

(B) Immunohistochemistry for CD138 (Sindecan-1), ×400: A marked brown/chocolate-colored stain (intense positivity) is observed predominantly on the plasma membrane of almost all the cells present, confirming the plasma cell origin of the neoplasm and enabling the degree of tumor infiltration in the bone marrow to be assessed. In this case, the findings indicated a plasma cell neoplasia, with CD138+, CD38+, κ+, λ−; pan-cytokeratin−, CD45 (LCA)−, CD20−, CD3−; Ki-67 ≈ 60% (Kappa-restricted plasma cell neoplasm).

| Timepoint | Event | Diagnostic framework applied |
|---|---|---|
| 5 months before admission | Onset of medial right arm pain with progressive functional limitation and constitutional symptoms (weight loss, asthenia). | Clinical suspicion only; no formal criteria yet applied. |
| Admission | Physical examination: decreased right basal breath sounds, pain-related limitation of the right shoulder secondary to a pathological fracture of the proximal humerus, without neurological deficit. Laboratory work-up revealed: severe normocytic anemia (Hb: 7.8 g/dL); total Ca: 10.4 mg/dL (albumin-corrected 11.7 mg/dL; 13.0 mg/dL on hospital day 11; PTH suppressed); creatinine: 1.3 mg/dL (CrCl ≈ 45 mL/min); 24-h proteinuria: 2,201 mg. | CRAB myeloma-defining events assessed per IMWG criteria [2]: C and A met; R not met. |
| Admission, imaging | Contrast-enhanced chest CT identifies a 6 cm osteolytic right 8th rib lesion with soft-tissue component (Figure 1A), plus additional lytic lesions elsewhere (such as the right humerus, scapulae, clavicles, ribs, sternum, vertebrae, sacrum, iliac bones, and left femoral neck); no pulmonary consolidation, nodules, or masses. The lesion was costal/extrapleural (6.0x3.5 cm) and, on MRI, extended to the adjacent vertebral body, considering an extrapleural paraskeletal soft-tissue component abutting the | IMWG imaging consensus: B met (multiplicity of lesions on CT argues against a solitary process); PET/CT or MRI recommended when a single lesion is in |

| | | |
|---|---|---|
| | pleura. | doubt [4]. |
| Admission, biomarkers | Serum protein electrophoresis/immunofixation: monoclonal IgA-kappa band (Figure 1B). SPEP: M-spike 2.9 g/dL (β region). Immunosubtraction: IgA-κ. IgA: 3,531 mg/dL; IgG: 329; IgM: 36.8 mg/dL. BM flow: 15.9% clonal κ plasma cells (CD38+/CD138+/CD45−/dim/CD19−/CD56−). Trephine CD138 IHC: 30%; CD56−, cyclin D1−, p53+ 30–40%. FLC, β2M, karyotype, iFISH: not available. | Biomarker criteria for MM vs. solitary plasmacytoma [2,6]. |
| Tissue diagnosis: Right 8th rib lesion, CT/US-guided core biopsy | Percutaneous biopsy of the rib lesion: kappa-restricted plasma cell neoplasm, CD138+, CD38+, κ+, λ−; pan-cytokeratin−, CD45 (LCA)−, CD20−, CD3−; Ki-67 ≈ 60% (Figure 2). | Minimum immunohistochemical requirement for plasma cell neoplasm diagnosis [6]. |
| Bone marrow (right posterior superior iliac spine) | 15.9% pathological plasma cells, cytoplasmic κ-restricted; CD38+, CD138+, CD45 negative/dim (intermediate in 38.3%), CD56−, CD19 negative (2.1% weakly positive), β2-microglobulin+. Background: neutrophil lineage 42.3%, erythroid 36%, T cells 3.3%, B cells 0.56% (polytypic κ:λ 1.9:1), NK cells 1.9% | Clonal plasma cell neoplasm with aberrant CD19−/CD45− phenotype; CD56-negative |
| Trephine biopsy — immunohistochemistry (B24-260) | CD138+ pathological plasma cells in multifocal clusters = 30% of total cellularity; monotypic κ, λ−; CD56−; cyclin D1−; p53 nuclear positivity in 30–40% of neoplastic cells (TP53 mutational study suggested) | BMPC 30% by CD138 IHC (vs. 15.9% by MFC); p53 overexpression; t(11;14) unlikely (cyclin D1−) |
| Conventional karyotype | No result in records | — |
| iFISH (CD138-selected) | Recommended: t(4;14) FGFR3::IGH, t(14;16) IGH::MAF, del(17p), 1p deletion/1q gain (CDKN2C/CKS1B) — not performed | Cytogenetic risk not assessable |
| TP53 sequencing | Not performed | — |
| Final classification | Polyostotic osteolytic pattern, ≥ 10% clonal BMPC and three MDEs (C, A, B) and absence of endobronchial/nodal disease support MM (IgA-k, Durie-Salmon IIIA) with underlying rib-based paraskeletal plasmacytoma rather than costal SBP or PPP. | IMWG diagnostic criteria; WHO 5th edition classification [1,2]. |
| Planned management | The records show that bortezomib-lenalidomide-dexamethasone (VRd) was prescribed but never administered; no radiotherapy was delivered to the rib or elsewhere; the patient died on day 67 after admission, under comfort-focused care. | Current MM management guidelines; ISS/R-ISS risk stratification [5,7]. |

**TABLE 1: Timeline of the diagnostic evaluation.**

The table maps the sequence of clinical, laboratory, imaging, and histopathological findings against the diagnostic framework applied at each step.

CRAB: hypercalcemia (C), renal impairment (R), anemia (A), and bone lesions (B); BM: bone marrow; BMPC: bone marrow plasma cells; β2M: beta-2 microglobulin; CD: cluster of differentiation; CK: cytokeratin; CrCl: creatinine clearance; CT: computed tomography; FLC: serum free light chains; Hb: hemoglobin; IgA, IgG, and IgM: immunoglobulin A, G, and M; IHC: immunohistochemistry; iFISH: interphase fluorescence in situ hybridization; IMWG: International Myeloma Working Group; ISS: International Staging System; κ: kappa light chain; λ: lambda light chain; L1: first lumbar vertebra; MFC: multiparameter flow cytometry; MDE: myeloma-defining event; MM: multiple myeloma; M-spike: monoclonal spike (monoclonal protein peak); PTH: parathyroid hormone; R-ISS: Revised International Staging System; SPEP: serum protein electrophoresis; VRd: bortezomib (Velcade), lenalidomide (Revlimid), and dexamethasone; WHO: World Health Organization; PPP, primary pulmonary plasmacytoma; SBP, solitary bone plasmacytoma.

Light-chain restriction was assessed by immunohistochemistry (kappa and lambda immunostains on formalin-fixed, paraffin-embedded tissue) in the rib biopsy, and by multiparameter flow cytometry (cytoplasmic kappa/lambda) together with trephine immunohistochemistry in the bone marrow; in situ hybridization was not performed. Bone marrow aspiration and trephine biopsy were performed from the right posterior superior iliac spine. Multiparameter flow cytometry of the aspirate identified 15.9% clonal plasma cells (CD38+, CD138+, CD45-negative/dim, CD19-negative, CD56-negative, cytoplasmic kappa-restricted), whereas CD138 immunohistochemistry on the trephine showed plasma cells in multifocal interstitial clusters accounting for 30% of the marrow cellularity, illustrating the known underestimation of plasma cell burden by flow cytometry.

The patient was considered ineligible for high-dose melphalan and autologous stem cell transplantation on the basis of age (75 years) and comorbidity, including chronic obstructive pulmonary disease with paraseptal emphysema (approximately 52 pack-years), multiple pathological fractures, and a Barthel index of 65 (Karnofsky 80%). Induction with bortezomib, lenalidomide, and dexamethasone (VRd) was prescribed: bortezomib 1.3 mg/m² (2.2 mg) subcutaneously on days 1, 8, 15, and 22; lenalidomide 15 mg orally on days 1-14 (renally adjusted); and dexamethasone 40 mg intravenously on days 1, 8, and 15, with aciclovir and

fluconazole prophylaxis. Hypercalcemia was managed with intravenous saline, furosemide, and dexamethasone 4 mg every eight hours; zoledronic acid 4 mg was prescribed but could not be administered owing to drug unavailability, as was denosumab. Iron deficiency was treated with intravenous iron sucrose, and monthly intravenous immunoglobulin (0.4 g/kg) was proposed for IgG hypogammaglobulinemia (IgG: 329 mg/dL).

Initiation of systemic therapy was deferred to allow curettage, cement augmentation, and intramedullary fixation of a pathological fracture of the right proximal humerus, with a 10-day wound-healing interval; an erector spinae plane block provided approximately 80% pain relief. On readmission for chemotherapy (two weeks ago), lenalidomide was unavailable at the institution. Contrast-enhanced thoracolumbar MRI showed diffuse cervical, thoracic, lumbar, and sacral lytic lesions, partial collapse of L1 with an epidural soft-tissue mass causing approximately 30% canal compromise and mild cauda equina compression, and a 59 × 38 × 38 mm mass of the right eighth rib extending into the adjacent vertebral body. Urgent spinal radiotherapy was requested for the L1 lesion; no radiotherapy was planned or delivered to the rib. Before radiotherapy could be given, the patient developed refractory hypercalcemia (14.4 mg/dL on hospital day 57), acute kidney injury (creatinine: 1.7 → 2.7 mg/dL; urea nitrogen: 42.8 mg/dL), hypernatremia (151.5 mmol/L), and hyperactive multifactorial delirium. On hospital day 60, in keeping with the patient's previously expressed reservations about treatment, his family requested comfort-focused care; the radiotherapy referral was withdrawn, and a do-not-resuscitate order was agreed. He died 67 days after admission, without having received myeloma-directed therapy; a hematological response could therefore not be assessed.

## Discussion

The main challenge in this case was the correct classification of the plasma cell lesion. Active MM is diagnosed when clonal bone marrow plasma cells account for at least 10% or a biopsy-proven plasmacytoma is present, together with one or more myeloma-defining events [1,2,5]. Our patient had 30% clonal bone marrow plasma cells on trephine immunohistochemistry (15.9% by flow cytometry), together with three myeloma-defining events: albumin-corrected hypercalcemia (11.7-13.0 mg/dL), anemia (hemoglobin: 7.8 g/dL), and multiple osteolytic lesions. Uncorrected total calcium (10.4 mg/dL) underestimated the true calcium burden because of hypoalbuminemia. Serum creatinine (1.3 mg/dL; creatinine clearance ≈ 45 mL/min) did not meet the IMWG renal threshold, and renal impairment was therefore not counted as a myeloma-defining event at diagnosis.

The presence of systemic disease excluded both SBP and PPP. Solitary plasmacytoma requires a single clonal lesion, no additional osteolytic lesions, and absent or minimal bone marrow involvement below 10% [2,6]. PPP is likewise a localized extramedullary neoplasm arising in the lung without evidence of MM [3,7]. Consequently, describing the lesion as a "solitary bone plasmacytoma with underlying MM" would be contradictory (Table *2*).

| Feature | Primary pulmonary plasmacytoma (PPP) | Solitary bone plasmacytoma (SBP) | Present case |
|---|---|---|---|
| Anatomical origin | Lung parenchyma | Single bone lesion | Right eighth (8th) rib |
| Bone marrow clonal plasma cells | <10% | <10% | 30% clonal plasma cells on trephine CD138 immunohistochemistry (15.9% by flow cytometry) |
| Additional osteolytic lesions | Absent | Absent | Present |
| Myeloma-defining event | Absent | Absent | Severe anemia and multiple bone lesions |
| Final classification | Localized extramedullary plasmacytoma | Localized bone plasmacytoma | MM with rib-based paraskeletal plasmacytoma |

**TABLE 2: Diagnostic features distinguishing primary pulmonary plasmacytoma, solitary bone plasmacytoma, and multiple myeloma with a rib-based paraskeletal plasmacytoma.**

The comparison summarizes the anatomical origin, bone marrow findings, presence of additional osteolytic lesions, myeloma-defining events, and final diagnostic classification relevant to the reported case.

The anatomical origin of the mass was essential for its interpretation. Plasma cell tumors extending directly from an osteolytic lesion into adjacent soft tissues are classified as paraskeletal or bone-associated plasmacytomas. This pattern differs from true extramedullary disease, which occurs in soft tissues without direct contact with bone [3,7]. In this patient, the osteolytic epicenter in the right eighth rib and the

contiguous pleuropulmonary component favored a rib-based paraskeletal plasmacytoma rather than a primary pulmonary lesion. Computed tomography is useful for identifying cortical destruction and defining the relationship between the rib, pleura, and lung. Bone-window images and multiplanar reconstructions may help establish the anatomical epicenter. However, whole-body low-dose CT, MRI, or 18F-fluorodeoxyglucose (18F-FDG) PET/CT is recommended to identify additional skeletal or marrow involvement [4,8]. In this case, the additional osteolytic lesions detected on conventional imaging were sufficient to exclude a solitary process, although PET/CT could have improved staging and provided a baseline for response assessment.

No cytogenetic or molecular risk stratification could be performed: interphase fluorescence in situ hybridization and TP53 sequencing were recommended by the hematopathology service but were not carried out, and conventional karyotyping yielded no reportable result in the record. Serum β2-microglobulin was requested but not resulted; therefore, International Staging System (ISS) and Revised International Staging System (R-ISS) stages could not be formally assigned, although the serum albumin of 2.4 g/dL excludes ISS stage I. The patient was classified as Durie-Salmon stage IIIA. Several surrogate markers nevertheless pointed to biologically aggressive disease: nuclear p53 overexpression in 30-40% of neoplastic plasma cells, which has been associated with TP53 alteration; a Ki-67 index of 60-70% in both osseous lesions; a CD56-negative, CD19-negative, CD45-negative/dim immunophenotype, CD56 loss having been linked to reduced marrow adhesion and a propensity for extramedullary/paraskeletal growth; IgA isotype; marked immunoparesis (IgG: 329 mg/dL); and PTH-independent hypercalcemia. Cyclin D1 negativity argues against t(11;14).

Histopathology confirmed a CD38-positive, kappa-restricted plasma cell neoplasm, while the monoclonal IgA-kappa component and clonal bone marrow infiltration demonstrated systemic disease. This distinction has direct therapeutic implications: localized plasmacytomas may be treated predominantly with radiotherapy, whereas MM requires systemic therapy, with local radiotherapy reserved for pain, neurological compromise, structural instability, or persistent bulky disease [5,9]. This case illustrates that a plasma cell mass located at the costopleural interface may resemble a pulmonary lesion, but its anatomical epicenter and the extent of systemic involvement determine its final classification, treatment, and prognosis.

## Conclusions

Differentiating SBP from PPP is a genuine diagnostic challenge, particularly when a lesion arises in an anatomically borderline location adjacent to the lung, as in the case presented here. Applying IMWG diagnostic criteria and, where available, PET/CT and clonotyping data allows this distinction to be made more rigorously than on radiological grounds alone. PPP characteristically presents with dyspnea, cough, hemoptysis, and regional lymph node involvement, and is generally curable with resection and/or radiotherapy, whereas SBP more often manifests with rib or vertebral pain, achieves comparable local control with radiotherapy but carries a substantially higher risk of progression to MM, and therefore warrants long-term surveillance and formal ISS/R-ISS staging once MM is confirmed. Histopathological and immunohistochemical findings are confirmatory for both entities, but correlation with clinical presentation, imaging, and IMWG laboratory criteria for MM remains essential to reach the correct diagnosis and to select the appropriate therapy.

Plasma cell tumors arising at the costopleural interface may be difficult to classify because a rib-based lesion with contiguous soft-tissue extension can resemble a primary pulmonary mass. In this case, the osteolytic rib lesion, additional skeletal involvement, severe anemia, and 30% clonal plasma cells on trephine CD138 immunohistochemistry (15.9% by flow cytometry) established the diagnosis of active MM with a rib-based paraskeletal plasmacytoma. Integration of anatomical imaging, histopathology, monoclonal protein studies, and bone marrow evaluation is essential to avoid misclassification as a solitary or primary pulmonary plasmacytoma, as this distinction directly determines staging and treatment.

## Additional Information

### Author Contributions

All authors have reviewed the final version to be published and agreed to be accountable for all aspects of the work.

**Concept and design:** Julián Rondón-Carvajal, Elena Useche-Henao, María José Espir-Sánchez, Yineth Agudelo-Zapata

**Acquisition, analysis, or interpretation of data:** Julián Rondón-Carvajal, Elena Useche-Henao, María José Espir-Sánchez, Yineth Agudelo-Zapata

**Drafting of the manuscript:** Julián Rondón-Carvajal, Elena Useche-Henao, María José Espir-Sánchez, Yineth Agudelo-Zapata

**Critical review of the manuscript for important intellectual content:** Julián Rondón-Carvajal, Elena

Useche-Henao, María José Espir-Sánchez, Yineth Agudelo-Zapata

**Supervision:** Julián Rondón-Carvajal, Elena Useche-Henao, María José Espir-Sánchez, Yineth Agudelo-Zapata

## Disclosures

**Human subjects:** Informed consent for treatment and open access publication was obtained or waived by all participants in this study. Ethics Committee - Hospital General de Medellín issued approval MI-DSI-IV00IF10. **Conflicts of interest:** In compliance with the ICMJE uniform disclosure form, all authors declare the following: **Payment/services info:** All authors have declared that no financial support was received from any organization for the submitted work. **Financial relationships:** All authors have declared that they have no financial relationships at present or within the previous three years with any organizations that might have an interest in the submitted work. **Other relationships:** All authors have declared that there are no other relationships or activities that could appear to have influenced the submitted work.

## Acknowledgements

The authors thank Dr. Guillermo Vélez, Professor of Radiology at CES University, for his assistance with image selection, and Hospital General de Medellín for granting permission to publish this clinical case.

# References

1. Alaggio R, Amador C, Anagnostopoulos I, et al.: The 5th edition of the World Health Organization Classification of Haematolymphoid Tumours: Lymphoid Neoplasms. Leukemia. 2022, 36:1720-48. 10.1038/s41375-022-01620-2
2. Rajkumar SV, Dimopoulos MA, Palumbo A, et al.: International Myeloma Working Group updated criteria for the diagnosis of multiple myeloma. Lancet Oncol. 2014, 15:538-48. 10.1016/S1470-2045(14)70442-5
3. Bladé J, Beksac M, Caers J, et al.: Extramedullary disease in multiple myeloma: a systematic literature review. Blood Cancer J. 2022, 12:45. 10.1038/s41408-022-00643-3
4. Hillengass J, Usmani S, Rajkumar SV, et al.: International Myeloma Working Group consensus recommendations on imaging in monoclonal plasma cell disorders. Lancet Oncol. 2019, 20:302-12. 10.1016/S1470-2045(19)30309-2
5. Rajkumar SV: Multiple myeloma: 2024 update on diagnosis, risk-stratification, and management . Am J Hematol. 2024, 99:1802-24. 10.1002/ajh.27422
6. Caers J, Paiva B, Zamagni E, et al.: Diagnosis, treatment, and response assessment in solitary plasmacytoma: updated recommendations from a European Expert Panel. J Hematol Oncol. 2018, 11:10. 10.1186/s13045-017-0549-1
7. Bansal R, Rakshit S, Kumar S: Extramedullary disease in multiple myeloma . Blood Cancer J. 2021, 11:161. 10.1038/s41408-021-00527-y
8. Palumbo A, Avet-Loiseau H, Oliva S, et al.: Revised international staging system for multiple myeloma: a report from International Myeloma Working Group. J Clin Oncol. 2015, 33:2863-9. 10.1200/JCO.2015.61.2267
9. Tsang RW, Campbell BA, Goda JS, et al.: Radiation therapy for solitary plasmacytoma and multiple myeloma: guidelines from the International Lymphoma Radiation Oncology Group. Int J Radiat Oncol Biol Phys. 2018, 101:794-808. 10.1016/j.ijrobp.2018.05.009